Korean Journal of Physiology and Pharmacology, Volume 28, Issue 2, 2024 DOI:10.25463/kjpp.28.2.2024.1
ISSN:1226-4512

Drug Ligand Interaction Between A.Baumannii Ptk Gene With The Bio-Active Compounds From The A.Indica

Karthik.V, Dr. Smiline Girija. A.S, Mrs.Shoba Gunasekaran, Dr.J.Vijayashree Priyadharsini J
Scholar, Bachelor of dental surgery, Chennai, Tamil Nadu, India.
Department of Microbiology, Saveetha Dental College and Hospitals Saveetha Institute of Medical and Technical Sciences, Saveetha university, Chennai, Tamil Nadu, India.
Department of Biotechnology, DG Vaishnav College, Arumbakkam, Chennai – 600 106
BRULAC-DRC, Saveetha Dental College and Hospitals, Saveetha Institute of Medical and Technical Sciences [SIMATS], Saveetha University, P.H.Road, Chennai, Tamilnadu - 600077, India

Abstract
Background: Over a period of time, there is an enormous increase in antibiotic resistance among bacteria due to evolution, adaptation, and overuse of synthetic drugs against them. Hence, there is always a need of developing potent antimicrobial drugs against them, and due to huge plant diversity and phytochemicals possessing secondary metabolites having antimicrobial activity, it can be a great alternative for synthetic drugs.The main aim of this current study was to analyze comparatively the interactions between bioactive compounds from Azadirachta indica and control drug ceftazidime by using the AutoDock program.
Materials and methods: The crystal structure of the structure of ptk was modeled using swissmodel server with further optimization of both the protein and ligands. In-silico inhibitory potential of the selected ligands against ptk was done by AutoDock 2.0 and was visualized with Accelrys Discovery Studio Visualizer tool with the assessment of the molecular properties of the ligands by molinspiration calculations and further assessment for their drug likeness.
Results: The amino acids of PTK binding with tyramine and Dehydrodiisoeugenol scored a promising inhibitory effect against PTK with a binding energy of -8.97 kcal/mol and -7.1 kcal/mol with 6 and 4 hydrogen bond interactions respectively when compared to ceftazidime with, –7.85 Kcal/mol with 11 hydrogen bond interactions.. Molinspiration assessments showed zero violations with TPSA values < 140 Å towards the best oral bioavailability.
Conclusion: Targeting the Inhibitors of biofilm forming genes like ptk of Acinetobacter baumannii had re-established the interest in recent years. The molecular docking results has shown the Successful inhibitory effect of bio active compounds of Azadirachta indica against the ptk gene of multiple drug resistant Acinetobacter baumannii. We hope the comprehensive structural understanding, binding modes and the vital factors affecting the binding free energies gotten from the present computational studies will provide valuable insights for future rational structure-based design of novel and potent inhibitors.

Keywords: Antimicrobial agents, ptk, Azadirachta indica, Acinetobacter baumannii, biofilm.

I. INTRODUCTION

Acinetobacter baumannii is a gram negative bacterium and an opportunistic pathogen in humans. It is mainly concerned with affecting the immune compromised people. The motility of the *Acinetobacter baumannii* is due to type 4 pili and also due to excretion of exopolysaccharide, which creates a bio-film which has high molecular weight sugar chains back of the bacteria which make it move forward [1]. Acinetobacter species mainly have efflux pumps which have the ability of removing a wide range of antimicrobial agents from the bacterial cell [2]. *ptk* of *Acinetobacter baumannii* plays a major role in capsule formation. In general, *ptk* homologues from gram-negative bacteria are integral membrane proteins harboring two transmembrane domains flanking a large periplasmic loop and have a cytoplasmic C-terminal region with Walker A and Walker B ATP-binding motifs and a tyrosine-rich C terminus where tyrosine phosphorylation occurs. In contrast, in gram-positive bacteria, the *ptk* homologues are present in two separate proteins, exhibiting significant sequence similarity to the two halves of the single peptides from gram-negative bacteria, and both proteins are required for phosphorylation [3,4]. Review of previous research had shown that *Acinetobacter* is Multidrug-resistant, that is it is resistant to antimicrobial agents like penicillin, cephalosporins, fluoroquinolones and aminoglycoside [5,6]. Since it is drug resistant, our current research focuses on a traditional way of formulating drugs which inhibits the activity of the bacterium. In the present study, we mainly focus over the compounds derived from *Azadirachta Indica* which is nothing but neem and particularly certain ligand is focused, like: Bis Phthalate, dehydrodi isoeugenol, 1-N-phenethyl ethanimine, MethylEthyl6-3-methyl-4-oxo-5,6,7-tetrahydro indole-2-carboxylate,ethyl 6,8-difluoro-4-hydroxyquinoline-3-carboxylate. Neem shows antimicrobial role through inhibitory effect on microbial growth/potentiality of cell wall breakdown. The neem nanoemulsion exhibited antibacterial activity against strains of bacterial pathogens by disrupting the integrity of the bacterial cell membrane. Different parts of the plant are shown to exhibit antimicrobial

effects against a broad range of microorganisms. Dehydrodi Isoeugenol acts as an antimicrobial compound at higher concentration [7,8].There is an enormous increase in antibiotic resistance among bacteria over a period of time due to evolution, adaptation, and overuse of synthetic drugs against them [9,10]. Hence, there is always a need of developing potent antimicrobial drugs against them, and due to huge plant diversity and phytochemicals possessing secondary metabolites having antimicrobial activity, it can be a great alternative for synthetic drugs [11].Previously our team has a rich experience in working on various research projects across multiple disciplines([12–26]. The main aim of this current study was to analyze comparatively the interactions between bioactive compounds (Imidazole-2-carboxylic acid, 4-methyl-,Bis(2-propyl-pentyl)phthalate,DehydrodiIsoeugenol,4-Hydroxy-N-(4,5-methylenedioxy-2-nitrobenzylidene)tyramine,Methylethyl6-(4-ethoxyphenyl)-3-methyl-4-oxo-5,6,7-tetrahydro indole-2-carboxylate,Ethyl 6,8-difluoro-4-hydroxyquinoline-3-carboxylate) from *Azadirachta indica* and control drug ceftazidime by using the AutoDock program.

II. METHODS:

2.1 Retrieval of *ptk* proteins and their optimization:

The crystal structure of *ptk* was retrieved from RCSB protein data bank (http://www.rcsb.org/pdb). Hydrogen atoms, solvation parameters and fragmental volumes to the protein were added and electronic charges were assigned to the protein atoms using kollman united atoms force field by using AutoDock Tool (ADT) –2.0.

2.2. Ligand preparation and optimisation:

Using Chemsketch Software the structures of the Biphthalate , dehydrodi isoeugenol 1-N-phenethyl ethanimine,Methylethyl 6-3-methyl-4-oxo-5,6,7-tetrahydro indole-2-carboxylate,ethyl 6,8-difluoro-4-hydroxyquinoline-3-carboxylate were drawn together with the generation of their 3-D structures and optimization. The selected ligands were retrieved in SDB format which were further saved in.mol file followed by the subsequent conversion using open babel molecular converter program [27] and were saved in PDB format.

2.3. Molinspiration assessment of the molecular properties of the selected compounds

The physicochemical and the pharmacological properties such as logP, hydrogen bond donor and acceptor characteristics, molecular size and rotatable bonds for (Bispthalate , dehydrodiisoeugenol1-N-phenethylmethanimine,Methylethyl6-3-methyl-4-oxo-5,6,7-tetrahydro indole-2-carboxylate,ethyl 6,8-difluoro-4-hydroxyquinoline-3-carboxylate)were predicted by molinspiration server [28]. Based on the Lipinsky's rule of five [29] characterization of the absorption, distribution, metabolism and elimination (ADME) of the selected compounds with further assessments and estimations of the molecular properties of the selected ligands was assessed. Membrane permeability and bio-availability was also evaluated.

2.4. Docking simulations & interpretations:

The docking analysis to interpret the affinity between bioactive compounds (Imidazole-2-carboxylic acid,4-methyl-,Bis(2-propyl pentyl)phthalate, Dehydrodi Isoeugenol,4-Hydroxy-N-(4,5-methylenedioxy-2-nitrobenzylidene)tyramine,Ethyl6,8-difluoro-4-hydroxyquinoline-3-carboxylate,)from *Azadirachta indica* against *ptk* gene of *Acinetobacter baumannii* , was achieved by auto-dock tool with the intermediary steps such as pdb.qt files for the proteins and the ligands. Using the graphical user interface program Auto-Dock tool (ADT) the grid box creation was completed with a grid size of 126x126x126 xyz points. Using Lamarckian genetic algorithm (LGA), docking simulation was achieved by setting the initial position, orientation and torsions of the ligand molecules in a random position. 10 different runs set to terminate after a maximum of 250,000 energy evaluations was used for each docking experiment with the population size set at 150. A translational step of 0.2 Å, quaternion and torsion steps of 5 were applied for each dock. The most favorable free energy of binding is achieved by clustering the results > 1.0 Å in positional root-mean-square deviation (RMSD). Finally, the pose was extracted and aligned with the receptor structure with the lowest binding energy or binding affinity for final analysis.

2.5. Docking visualization :

The protein-ligand interactions like hydrogen bonding and other non-bonded energies between (Bispthalate,dehydrodiisoeugenol1-N-phenethylmethanimine,Methylethyl6-3-methyl-4-oxo-5,6,7-tetrahydro indole-2-carboxylate,ethyl 6,8-difluoro-4-hydroxyquinoline-3-carboxylate) against *ptk* gene of *Acinetobacter baumannii* were visualized using Accelrys Discovery Studio Visualizer software that displays an output file and the binding area of the ligand at the surface of the protein. The relative stabilities were evaluated using their molecular dynamics, binding affinities, energy simulations with further docking score assessments.

III. RESULT

3.1 Structure retrieval of the *ptk* from *Acinetobacter baumannii.*

The crystal structure of *ptk* which was not available in PDB database. Hence modeled using swissmodel server using the template 3LA6.1.A (figure 3). Moreover, the structure of *ptk* was plotted in Ramachandran plot and it also showed 88.4% of residues in most of the favoured region (figure 2). The sequence of *ptk* from the *Acinetobacter baumannii* was retrieved from Uniprot database and its sequence id was A0A171EWN0. Removal of the water molecules and final stage merging of hydrogen atoms to the receptor molecule was successful. The 3D structure of *ptk* was visualized using RASMOL with the analysis of pink color indicating the alpha-helix, yellow arrow indicating the beta sheets and white color indicating the turns (Figure 1).

 DOI:10.25463/kjpp.28.2.2024.1

Figure 1 RASMOL 3D structure of *ptk* gene

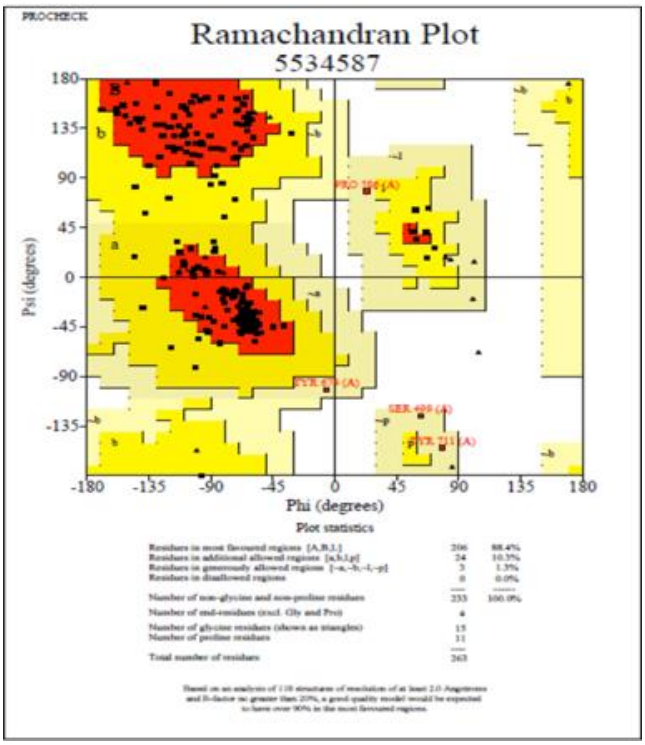

Figure 2 Ramachandran plot- Predicted using SAVES Server - PROCHECK

 DOI:10.25463/kjpp.28.2.2024.1

Figure 3 Structure Prediction of *ptk* by Homology modeling using Swissmodel server

3.2 Structure retrieval of the bio-active compounds from the *Azadirachta indica*:

The ligand optimization was achieved using ACD Chemsketch and retrieved in a compatible format using OpenBabel molecular converter tool. The retrieved 2D and 3D structures of the ligands and its SMILES format are shown in Table 1.

Compound name	2D	3D	SMILES	Mol formula
Imidazole-2-carboxylic acid, 4-methyl-	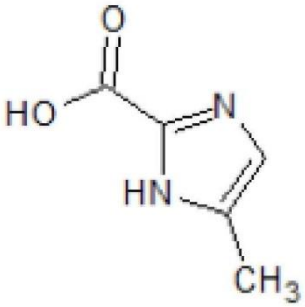	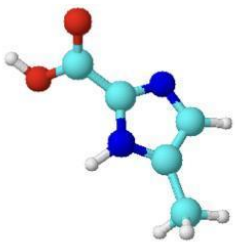	CC1=CN=C(N1)C(=O)O	$C_5H_6N_2O_2$
Bis(2-propyl pentyl) phthalate	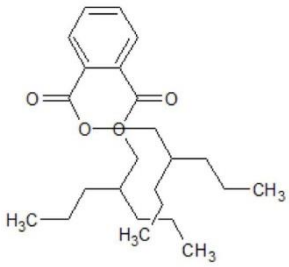	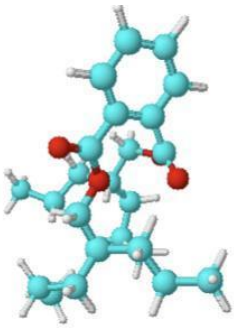	CCCC(CCC)COC(=O)C1=CC=CC=C1C(=O)OCC(CCC)CCC	$C_{24}H_{38}O_4$
Dehydrodi Isoeugenol	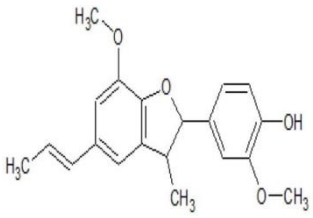	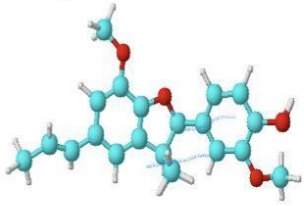	CC=CC1=CC2=C(C(=C1)OC)OC(C2C)C3=CC(=C(C=C3)O)OC	$C_{20}H_{22}O_4$

4-Hydroxy-N-(4,5-methylenedioxy-2-nitrobenzylidene)tyramine	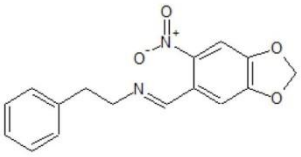	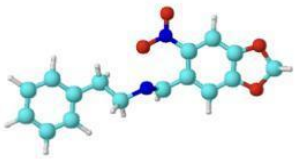	C1OC2=C(O1)C=C(C(=C2)C=NCCC3=CC=CC=C3)[N+](=O)[O-]	$C_{16}H_{14}N_2O_4$
Methyl Ethyl 6-(4-ethoxyphenyl)-3-methyl-4-oxo-5,6,7-tetrahydro indole-2-carboxylate	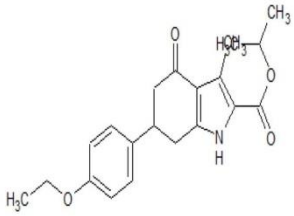	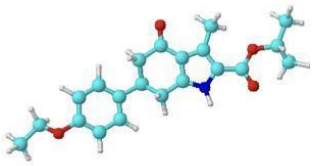	CCOC1=CC=C(C=C1)C2CC3=C(C(=C(N3)C(=O)OC(C)C)C)C(=O)C2	$C_{21}H_{25}NO_4$
Ethyl 6,8-difluoro-4-hydroxyquinoline-3-carboxylate	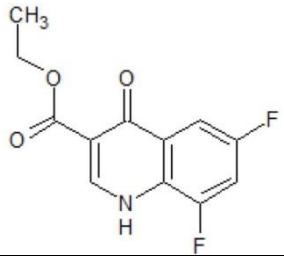	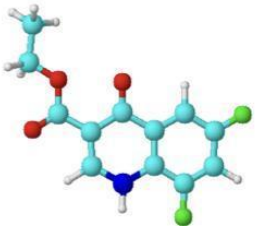	CCOC(=O)C1=CNC2=C(C1=O)C=C(C=C2F)F	$C_{12}H_9F_2NO_3$

Table 1: 2D and 3D structures and SMILES format of the bio-active compounds from the *Azadirachta indica* .

3.3 Molinspiration estimation towards drug likeness

The bioactivity scores prediction of bio-active compounds of *Azadirachta indica* against *ptk* of *Acinetobacter baumannii* . based on the calculation towards drug likeness is scored and tabulated in Table 2 . Molecular properties were calculated on the basis of Lipinski's rule of five and its components. From the molinspiration results, except phthalate which shows one violation, all the other compounds show n-violation values of 0, Hence all molecules satisfy Lipinski's Rule of 5. TPSA was <140 Å for all the compounds thus indicating its higher absorption and promising oral bioavailability.

Compounds	M.wt	Hydrogen Bond Donor	Hydrogen Bond Acceptor	miLog P	Rotatable bonds	nViolations	TPSA (Å)	Volume	N atoms
Imidazole-2-carboxylic acid, 4-methyl-	126.11	2	4	-0.17	1	0	65.98	104.44	9
Phthalate	390.56	0	4	8.04	16	1	52.61	407.90	28
Dehydrodi Isoeugenol	326.39	1	4	4.10	4	0	47.93	306.90	24
4-Hydroxy-N-(4,5-methylenedioxy-2-nitrobenzylidene)tyramine	298.30	0	6	3.35	5	0	76.66	259.58	22
Methyl Ethyl 6-(4-ethoxyphenyl)-3-methyl-4-oxo-5,6,7-tetrahydro indole-2-carboxylate	355.43	1	5	4.54	6	0	68.40	335.84	26

Ethyl 6,8-difluoro-4-hydroxyquinoline-3-carboxylate	253.20	1	4	0.10	3	0	59.17	203.20	18
Ceftazidime	546.59	4	13	–5.68	9	2	191.23	439.78	37

Table 2: Molinspiration calculations of bio-active compounds.

3.4 Docking analysis of the bio-active compounds from *Azadirachta indica* against the *ptk* gene of *Acinetobacter baumannii*.

The best conformers were selected using LGA based on the best ligand-receptor structure from the docked structure based on the lowest energy and minimal solvent accessibility. Accelrys Discovery Studio Visualizer tool of the hydrogen bond interactions in the stick model between bio-active compounds of *Azadirachta indica* and *ptk* of *Acinetobacter baumannii* is given in Figure-4. The amino acids of *ptk* binding with 4-Dihydroxy-N-(4,5-methylenedioxy-2-nitrobenzylidene)tyramine and Dehydrodiisoeugenol scored a promising inhibitory effect against PTK with a binding energy of -8.97 kcal/mol and -7.1 kcal/mol with 6 and 4 hydrogen bond interactions respectively when compared to ceftazidime with, –7.85 Kcal/mol with 11 hydrogen bond interactions.

The torsional energy and the docking scores between the drug and ligands are given in Table 3. It was evident from the docking analysis that bio-active compounds from *Azadirachta indica* possess more promising inhibitory action against *ptk* efflux pumps of *Acinetobacter baumannii*.

***Ptk* docking with compounds**	**Hydrogen bonds interactions**	**van der Waals interactions**	**π-σ interactions/ π-π T-shaped interactions/ amide-π stacked interactions**	**alkyl/π-alkyl interactions**	**π-anion interactions**
Imidazole-2-carboxylic acid, 4-methyl-	7	5	-	-	-
Bis(2-propyl pentyl) phthalate	1	4	-	3	1
Dehydrodi Isoeugenol	4	6	1	2	1
4-Hydroxy-N-(4,5-methylenedioxy-2-nitrobenzylidene)tyramine	6	8	2	-	-
Methyl Ethyl 6-(4-ethoxyphenyl)-3-methyl-4-oxo-5,6,7-tetrahydro indole-2-carboxylate	4	7	1	4	-
Ethyl 6,8-difluoro-4-hydroxyquinoline-3-carboxylate	7	5	-	2	-
Ceftazidime	11	4	-	2	-

Table 3: Overall docking results of bio-active compounds from *Azadirachta indica* against *ptk* gene of *Acinetobacter baumannii*.

 DOI:10.25463/kjpp.28.2.2024.1

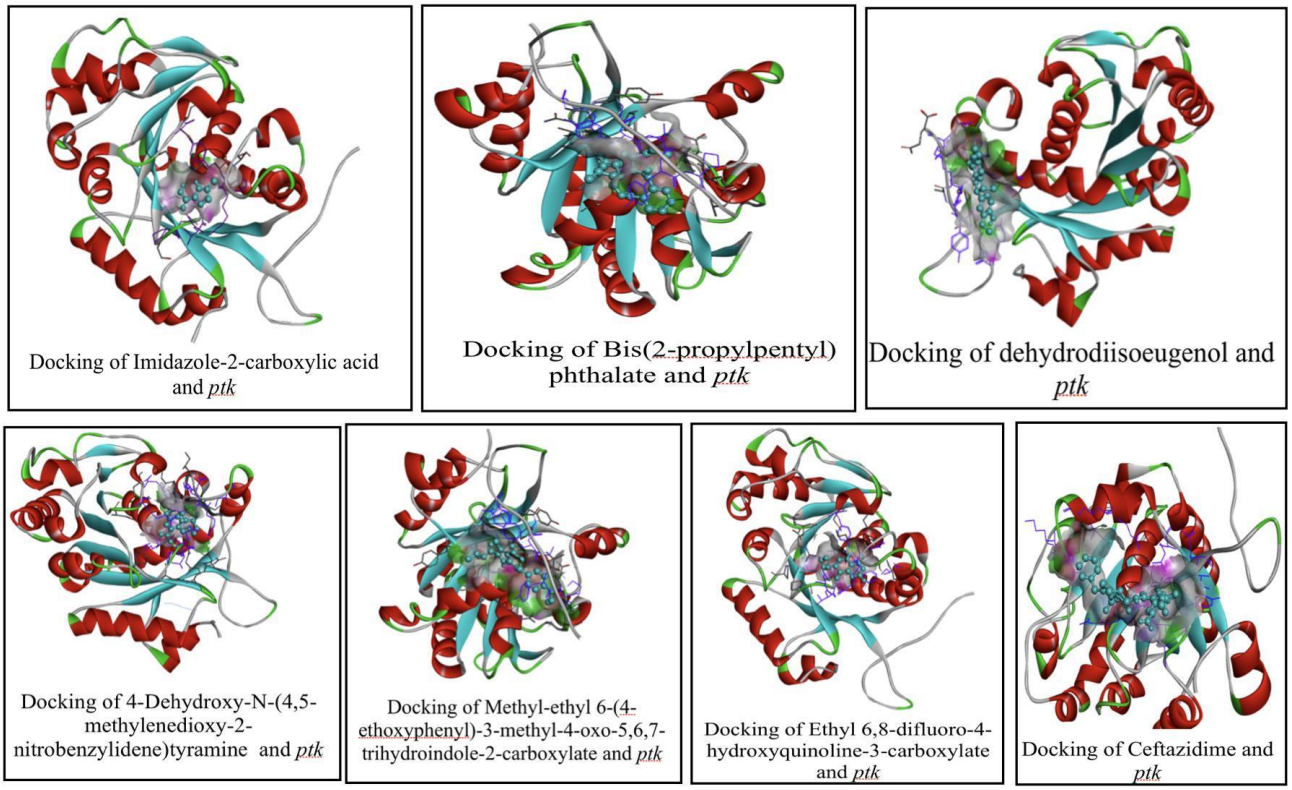

Figure 4: Accelrys discovery studio visualisation of the hydrogen interactions between bio-active compounds from *Azadirachta indica* against *ptk* of *Acinetobacter baumannii*.

IV. DISCUSSION:

There is an enormous increase in antibiotic resistance among bacteria over a period of time due to evolution, adaptation, and overuse of synthetic drugs against them, hence it's necessary to formulate a drug which targets the biofilm forming ability of these microbes . We have chosen the multiple drug resistant *Acinetobacter baumannii* and target the *ptk* gene which is mainly involved in the biofilm formation. It had shown that the *ptk* gene fits best with the bio-active compounds from *Azadirachta indica* was efficiently achieved in the investigation which was done by molecular docking analysis which is a molecular modeling technique [30].

The structure of *ptk* was not available in PDB database. Hence it was modeled using Swissmodel server using the template 3LA6.1.A Chain. The modeled structure was found to be highly plausible as it had 45.86% sequence identity with that of the template. Moreover, the Ramachandran plot also showed 88.4% of residues in most favored regions and with no residues in disallowed region. A promising receptor-ligand complex was obtained when the *ptk* gene was docked against the bio-active compounds from *Azadirachta indica*. In docking analysis there are two main steps, the strength of target-ligand binding interactions is achieved by scoring and the prediction of the exact orientation of the conformers into the best active site pocket called pose[31].

The molecular docking results had confirmed that the hydrogen bonding with these *ptk* have pivotal contributions to the binding structures and binding free energies, although the van der Waals and Pi-interactions contributed to the stabilization of the binding structures. We hope the comprehensive structural understanding, binding modes and the vital factors affecting the binding free energies gotten from the present computational studies will provide valuable insights for future rational structure-based design of novel and potent inhibitors . In this context, 4-Hydroxy-N-(4,5-methylenedioxy-2-nitrobenzylidene)tyramine shows six hydrogen bond interaction with *ptk* receptor with least binding energy of –8.97 Kcal/mol.Methylethyl6-(4-ethoxyphenyl)-3-methyl-4-oxo-5,6,7-tetrahydro indole-2-carboxylate and Dehydrodi Isoeugenol shows four hydrogen bond interaction with *ptk* receptor with least binding energy of –8.43 Kcal/mol and –7.1 Kcal/mol. Ethyl 6,8-difluoro-4-hydroxyquinoline-3-carboxylate and Imidazole-2-carboxylic acid, 4-methyl- shows seven hydrogen bonds with least binding energy of –6.33 Kcal/mol and –5.76 Kcal/mol. Bis(2-propyl pentyl) phthalate shows one hydrogen bond interaction with a ptk receptor with least binding energy of–3.62 Kcal/mol. All the six compound utilizes least energy with hydrogen bond formation and van der Waals interaction and the compound 4-Dihydroxy-N-(4,5-methylenedioxy-2-nitrobenzylidene)tyramine and Dehydrodiisoeugenol compounds utilizes least energy than control drug Ceftazidime which shows binding energy of –7.85 Kcal/mol.

Mol Inspirational calculations were done for this study to evaluate the likenesses of ligand. From the molinspiration results, except Bis(2-propyl pentyl)Phthalate which shows one violation, all the other compounds shows n-violation values of bioactive compounds are 0, Hence all molecules satisfy Lipinski's Rule of 5 and the control drug Ceftazidime shows two violation.

TPSA of all ligands exhibited 20.23 Å to 140 Å ranges, which indicates good bioavailability by oral route. The docking scores and the binding energy between bio-active compounds of *Azadirachta indica* and the *ptk* gene of *A.baumannii* had shown their potential towards antibacterial drug candidates which could have a strong action towards biofilm formation. Moreover, the study has its own limitations since we did not perform in-vitriol inhibitory bioassay Our institution is passionate about high quality evidence based research and has excelled in various fields [32–38]. We hope this study adds to this rich legacy.

V. CONCLUSION

Targeting the inhibitors of biofilm forming genes like *ptk* of *Acinetobacter baumannii* had re-established the drug interest in recent years. The molecular docking results has shown the successful inhibitory effect of bio-active compounds of *Azadirachta indica* against the *ptk* gene of multiple drug resistant *A.baumannii*. We hope the comprehensive structural understanding, binding modes and the vital factors affecting the binding free energies obtained from the present computational study will provide valuable insights for future rational structure-based design of novel and potent inhibitors for *A.baumannii*.

VI. AUTHOR CONTRIBUTIONS :

Idea and study was conceptualized by Dr. Smiline Girija. A.S, collection of the literature and drafting the manuscript was done by Karthik, revising of the manuscript was done by Dr.J.Vijayashree Priyadharsini J. Execution and analysis of results was done by Mrs.Shoba Gunasekaran.

VII. CONFLICT OF INTEREST :

The authors declare no conflict of interest

REFERENCE:

1. McQueary CN, Kirkup BC, Si Y, et al. Extracellular stress and lipopolysaccharide modulate Acinetobacter baumannii surface-associated motility. *Journal of Microbiology* 2012; 50: 434–443.
2. Bonomo RA, Szabo D. Mechanisms of Multidrug Resistance in Acinetobacter Species and Pseudomonas aeruginosa. *Clinical Infectious Diseases* 2006; 43: S49–S56.
3. Fattahian Y, Rasooli I, Gargari SLM, et al. Protection against Acinetobacter baumannii infection via its functional deprivation of biofilm associated protein (Bap). *Microbial Pathogenesis* 2011; 51: 402–406.
4. Aliramezani A, Douraghi M, Hajihasani A, et al. Clonal relatedness and biofilm formation of OXA-23-producing carbapenem resistant Acinetobacter baumannii isolates from hospital environment. *Microbial Pathogenesis* 2016; 99: 204–208.
5. Simor AE, Lee M, Vearncombe M, et al. An Outbreak Due to MultiresistantAcinetobacter baumanniiin a Burn Unit: Risk Factors for Acquisition and Management. *Infection Control & Hospital Epidemiology* 2002; 23: 261–267.
6. Gusten WM, Hansen EA, Cunha BA. Acinetobacter baumannii pseudomeningitis. *Heart & Lung* 2002; 31: 76–78.
7. Perkins EG. Characterization of the nonvolatile compounds formed during the thermal oxidation of corn oil. II. Phthalate esters. *Journal of the American Oil Chemists' Society* 1967; 44: 197–199.
8. Nguyen D, Nguyen D, La LH, et al. Isolation of dioctyl phthalate with high depigmenting effect from Chinese herb Nigella glandulifera Freyn. *Journal of Biotechnology* 2007; 131: S43.
9. Ruan H-L, Zhou X-F, Zhang Y-H, et al. Ferulic acid esters from Euphorbia hylonoma. *Fitoterapia* 2007; 78: 72–73.
10. Akhand M, Al-Bari MAA, Islam MA, et al. Characterization and Antimicrobial Activities of a Metabolite from a New *Streptomyces* Species from Bangladeshi Soil. *Journal of Scientific Research* 2009; 2: 178–185.
11. Murakami Y, Shoji M, Hirata A, et al. Dehydrodiisoeugenol, an isoeugenol dimer, inhibits lipopolysaccharide-stimulated nuclear factor kappa B activation and cyclooxygenase-2 expression in macrophages. *Archives of Biochemistry and Biophysics* 2005; 434: 326–332.
12. Neelakantan P, Sharma S, Shemesh H, et al. Influence of Irrigation Sequence on the Adhesion of Root Canal Sealers to Dentin: A Fourier Transform Infrared Spectroscopy and Push-out Bond Strength Analysis. *J Endod* 2015; 41: 1108–1111.
13. Sathish T, Karthick S. Wear behaviour analysis on aluminium alloy 7050 with reinforced SiC through taguchi approach. *J Jpn Res Inst Adv Copper-Base Mater Technol* 2020; 9: 3481–3487.
14. Patil SB, Durairaj D, Suresh Kumar G, et al. Comparison of Extended Nasolabial Flap Versus Buccal Fat Pad Graft in the Surgical Management of Oral Submucous Fibrosis: A Prospective Pilot Study. *J Maxillofac Oral Surg* 2017; 16: 312–321.
15. Abdul Wahab PU, Senthil Nathan P, Madhulaxmi M, et al. Risk Factors for Post-operative Infection Following Single Piece Osteotomy. *J Maxillofac Oral Surg* 2017; 16: 328–332.
16. Eapen BV, Baig MF, Avinash S. An Assessment of the Incidence of Prolonged Postoperative Bleeding After Dental Extraction Among Patients on Uninterrupted Low Dose Aspirin Therapy and to Evaluate the Need to Stop Such Medication Prior to Dental Extractions. *J*

Maxillofac Oral Surg 2017; 16: 48–52.
17. Wahab PUA, Madhulaxmi M, Senthilnathan P, et al. Scalpel Versus Diathermy in Wound Healing After Mucosal Incisions: A Split-Mouth Study. *J Oral Maxillofac Surg* 2018; 76: 1160–1164.
18. Jeevanandan G, Govindaraju L. Clinical comparison of Kedo-S paediatric rotary files vs manual instrumentation for root canal preparation in primary molars: a double blinded randomised clinical trial. *European Archives of Paediatric Dentistry* 2018; 19: 273–278.
19. Samuel SR, Acharya S, Rao JC. School Interventions-based Prevention of Early-Childhood Caries among 3-5-year-old children from very low socioeconomic status: Two-year randomized trial. *J Public Health Dent* 2020; 80: 51–60.
20. Mehta M, Deeksha, Tewari D, et al. Oligonucleotide therapy: An emerging focus area for drug delivery in chronic inflammatory respiratory diseases. *Chem Biol Interact* 2019; 308: 206–215.
21. Ezhilarasan D, Sokal E, Najimi M. Hepatic fibrosis: It is time to go with hepatic stellate cell-specific therapeutic targets. *Hepatobiliary Pancreat Dis Int* 2018; 17: 192–197.
22. Rajeshkumar S, Menon S, Venkat Kumar S, et al. Antibacterial and antioxidant potential of biosynthesized copper nanoparticles mediated through Cissus arnotiana plant extract. *Journal of Photochemistry and Photobiology B: Biology* 2019; 197: 111531.
23. Ravindiran M, Praveenkumar C. Status review and the future prospects of CZTS based solar cell – A novel approach on the device structure and material modeling for CZTS based photovoltaic device. *Renewable Sustainable Energy Rev* 2018; 94: 317–329.
24. Ramamoorthi S, Nivedhitha MS, Divyanand MJ. Comparative evaluation of postoperative pain after using endodontic needle and EndoActivator during root canal irrigation: A randomised controlled trial. *Aust Endod J* 2015; 41: 78–87.
25. Malli Sureshbabu N, Selvarasu K, V JK, et al. Concentrated Growth Factors as an Ingenious Biomaterial in Regeneration of Bony Defects after Periapical Surgery: A Report of Two Cases. *Case Rep Dent* 2019; 2019: 7046203.
26. Manivannan I, Ranganathan S, Gopalakannan S, et al. Tribological and surface behavior of silicon carbide reinforced aluminum matrix nanocomposite. *Surf Interfaces* 2017; 8: 127–136.
27. O'Boyle NM, Banck M, James CA, et al. Open Babel: An open chemical toolbox. *Journal of Cheminformatics*; 3. Epub ahead of print 2011. DOI: 10.1186/1758-2946-3-33.
28. Jarrahpour A, Fathi J, Mimouni M, et al. Petra, Osiris and Molinspiration (POM) together as a successful support in drug design: antibacterial activity and biopharmaceutical characterization of some azo Schiff bases. *Medicinal Chemistry Research* 2012; 21: 1984–1990.
29. Lipinski CA, Lombardo F, Dominy BW, et al. Experimental and computational approaches to estimate solubility and permeability in drug discovery and development settings 1PII of original article: S0169-409X(96)00423-1. The article was originally published in Advanced Drug Delivery Reviews 23 (1997) 3–25. 1. *Advanced Drug Delivery Reviews* 2001; 46: 3–26.
30. Nakai H, Tang Y, Gantzel P, et al. A new entry to N-heterocyclic carbene chemistry: synthesis and characterisation of a triscarbene complex of thallium(i). *Chem. Commun.* 2003; 24–25.
31. Lee E-W, Nazmul Huda M, Kuroda T, et al. EfrAB, an ABC Multidrug Efflux Pump in Enterococcus faecalis. *Antimicrobial Agents and Chemotherapy* 2003; 47: 3733–3738.
32. Vijayashree Priyadharsini J. In silico validation of the non-antibiotic drugs acetaminophen and ibuprofen as antibacterial agents against red complex pathogens. *J Periodontol* 2019; 90: 1441–1448.
33. Ezhilarasan D, Apoorva VS, Ashok Vardhan N. Syzygium cumini extract induced reactive oxygen species-mediated apoptosis in human oral squamous carcinoma cells. *J Oral Pathol Med* 2019; 48: 115–121.
34. Ramesh A, Varghese S, Jayakumar ND, et al. Comparative estimation of sulfiredoxin levels between chronic periodontitis and healthy patients - A case-control study. *J Periodontol* 2018; 89: 1241–1248.
35. Mathew MG, Samuel SR, Soni AJ, et al. Evaluation of adhesion of Streptococcus mutans, plaque accumulation on zirconia and stainless steel crowns, and surrounding gingival inflammation in primary …. *Clin Oral Investig*, https://link.springer.com/article/10.1007/s00784-020-03204-9 (2020).
36. Sridharan G, Ramani P, Patankar S, et al. Evaluation of salivary metabolomics in oral leukoplakia and oral squamous cell carcinoma. *J Oral Pathol Med* 2019; 48: 299–306.
37. Pc J, Marimuthu T, Devadoss P. Prevalence and measurement of anterior loop of the mandibular canal using CBCT: A cross sectional study. *Clin Implant Dent Relat Res*, https://europepmc.org/article/med/29624863 (2018).
38. Ramadurai N, Gurunathan D, Samuel AV, et al. Effectiveness of 2% Articaine as an anesthetic agent in children: randomized controlled trial. *Clin Oral Investig* 2019; 23: 3543–3550.